NJC

# μ–Nitrido-Bridged Iron Phthalocyanine Dimer Bearing Eight Peripheral 12-Crown-4 Units and Its Methane Oxidation Activity

| | |
|---|---|
| Journal: | *New Journal of Chemistry* |
| Manuscript ID | NJ-ART-09-2020-004601.R1 |
| Article Type: | Paper |
| Date Submitted by the Author: | 25-Oct-2020 |
| Complete List of Authors: | Yamada, Yasuyuki; Nagoya University, Research Center for Materials Science<br>Kura, Jyunichi; Nagoya University, Department of Chemistry<br>Toyoda, Yuka; Nagoya University, Department of Chemistry<br>Tanaka, Kentaro; Nagoya University, Department of Chemistry, Graduate School of Science |
| | |

PAPER

# μ–Nitrido-Bridged Iron Phthalocyanine Dimer Bearing Eight Peripheral 12-Crown-4 Units and Its Methane Oxidation Activity

Received 00th January 20xx,
Accepted 00th January 20xx

DOI: 10.1039/x0xx00000x

Yasuyuki Yamada,*[a,b,c] Jyunichi Kura,[b] Yuka Toyoda,[b] and Kentaro Tanaka *[a]

A novel μ-nitrido-bridged iron phthalocyanine dimer with eight peripheral 12-crown-4 units as an electron-donating substituent was synthesized and characterized. Examination of its methane oxidation activity in the presence of $H_2O_2$ in an acidic aqueous solution suggested that the high-valent iron oxo species generated *in situ* was unstable and the transiently generated decomposed species showed methane oxidation activity *via* Fenton-type reaction.

## Introduction

Methane is a potential feedstock for next-generation chemicals because it is abundant in nature as natural gas or methane hydrate.[1,2] However, because of its high chemical stability, it is difficult to convert it into more valuable chemical raw materials under mild reaction conditions.[3,4] Therefore, the development of novel catalysts for efficient and easier chemical conversion of methane has been intensively studied. Although some potent catalysts based on metal oxides,[5] zeolites[6–9], or inorganic salts with light irradiation[10,11] have recently been developed, the number of molecular catalysts that can efficiently convert methane under mild reaction conditions is still limited.[12–17]

μ-Nitrido-bridged iron phthalocyanine dimer (**1**) is one of the most potent molecular catalysts for methane conversion under mild reaction conditions.[13–16] Both neutral species with Fe(III) and Fe(IV) ions (**1**) and a monocationic species containing two Fe(IV) ions (**1**$^+$) have been reported to oxidize methane to afford methanol, formaldehyde, and formic acid in an acidic aqueous solution in the presence of $H_2O_2$ below 100 °C (Figure 1a). The actual reactive species of **1** is its high-valent iron-oxo species (**1**$_{oxo}$) generated *in situ* (Figure 1b).[13,15] Moreover, it has been reported that the introduction of the electron-donating *tert*-butyl substituent to the phthalocyanine ring of μ-nitrido-bridged iron phthalocyanine dimer increased the methane oxidation rate, whereas the electron-

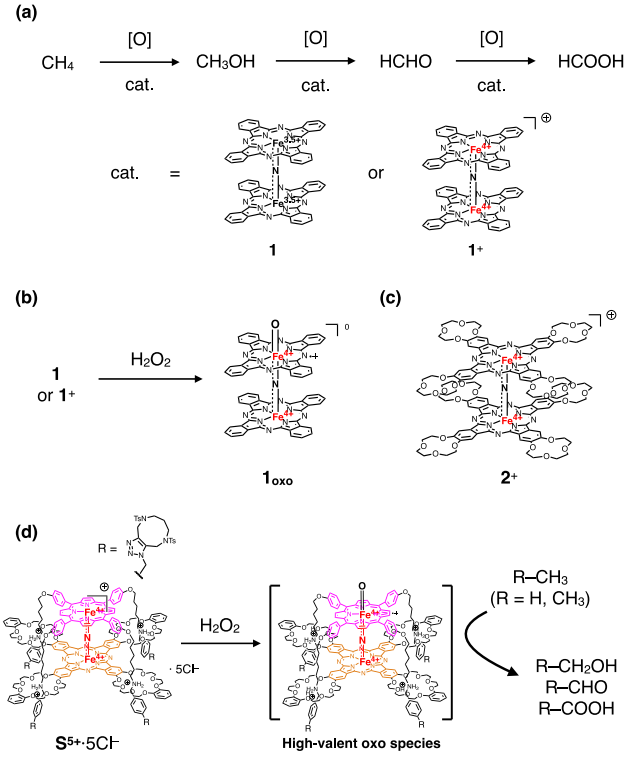


**Figure 1** (a) Stepwise methane oxidation catalyzed by μ-nitrido-bridged iron phthalocyanine dimers (**1** or **1**$^+$). (b) Generation of high-valent iron oxo species from **1** or **1**$^+$. (c) Structure of a monocationic μ-nitrido-bridged iron phthalocyanine dimer with eight peripheral 12-crown-4 units (**2**$^+$). (d) Catalytic oxidation reactions of methane and ethane by using a μ-nitrido-bridged dinuclear iron complex of a supramolecular cofacial assembly of a porphyrin and a phthalocyanine connected through four 24-crown-8–dialkylammonium rotaxanes.

[a] *Department of Chemistry, Graduate School of Science, Nagoya University, Furo-cho, Chikusa-ku, Nagoya 464-8602, Japan.*
[b] *Research Center for Materials Science, Nagoya University, Furo-cho, Chikusa-ku, Nagoya 464-8602, Japan.*
[c] *JST, PRESTO, 4-1-8 Honcho, Kawaguchi, Saitama, 332-0012, Japan.*
†*E-mail*: yy@chem.nagoya-u.ac.jp, kentaro@chem.nagoya-u.ac.jp
Electronic Supplementary Information (ESI) available: [details of any supplementary information available should be included here]. See DOI: 10.1039/x0xx00000x

withdrawing sulfonate substituent decreased it.[16] Therefore, it would be interesting to know whether other strong electron-donating substituents can increase the reaction rate of methane oxidation. However, the synthesis and electronic structure of the μ-nitrido-bridged iron phthalocyanine dimer with strong electron donating substituents such as alkoxy groups and its methane oxidation activities have not been investigated so far. Since the introduction of peripheral substituents to the phthalocyanine ring would strongly influence both the electronic structure and reactivity of μ-nitrido-bridged iron phthalocyanine dimers, more investigation should help advance the chemistry of μ-nitrido-bridged iron phthalocyanine dimers.

In this study, we designed a novel monocationic μ-nitrido-bridged iron phthalocyanine dimer bearing eight 12-crown-4 moieties (**2**$^+$ in Figure 1c). The 12-crown-4 units act as electron-donating groups. Moreover, it is promising that introduction of flexible 12-crown-4 units should increase the solubility of the μ-nitrido-bridged iron phthalocyanine dimer core in various organic solvents. This would be helpful for purification of **2**$^+$. It is also expected that the 12-crown-4 units would not interfere with the oxidation reaction involving the high-valent iron-oxo species of **2**$^+$ (**2**$_{oxo}$) since the 12-crown-4 units of **2**$_{oxo}$ would not reach the iron-oxo center, as revealed by molecular modeling (Figure S1 in the Supporting Information). We recently demonstrated that catalytic methane and ethane oxidation reactions proceeded successfully by using a high-valent iron-oxo species of a μ-nitrido-bridged dinuclear iron complex of a supramolecular cofacial assembly of a porphyrin and a phthalocyanine connected through four 24-crown-8–dialkylammonium rotaxanes (Figure 1d).[17,18] These suggested that peripheral crown ether units of the catalyst would not interfere the reaction of high-valent iron-oxo species as long as they can not reach the reaction center. Based on these considerations, we decided to investigate the electronic structure of **2**$^+$ as well as its catalytic methane oxidation activity under mild reaction condition in the presence of $H_2O_2$ as an oxidant.

## Results and Discussion

The synthetic procedure for **2**$^+$ is summarized in Figure 2a. 4,5-Dicyanobenzo-12-crown-4[19] was heated in the presence of $Fe(OAc)_2$ in *N*,*N*-dimethylaminoethanol to obtain Fe(II)-phthalocyanine **3** bearing four 12-crown-4 units in 63% yield. The formation of μ-nitrido-bridged iron phthalocyanine dimer was performed as described in our previous report on the synthesis of the phthalocyanine dimer with no peripheral substituent.[20] First, **3** was heated at 280 °C in 1-chloronaphthalene in the presence of excess $NaN_3$ under air. After successive oxidation by iodine followed by purification by silica-gel column chromatography and gel permeation chromatography, a monocationic species of the desired μ-nitrido-bridged iron phthalocyanine dimer **2**$^+$·I$^-$ was obtained in 20% isolated yield as a bluish-green solid.

$^1$H-NMR, MALDI-TOF MS, and UV-Vis spectroscopies and elemental analysis were performed to characterize **2**$^+$·I$^-$.

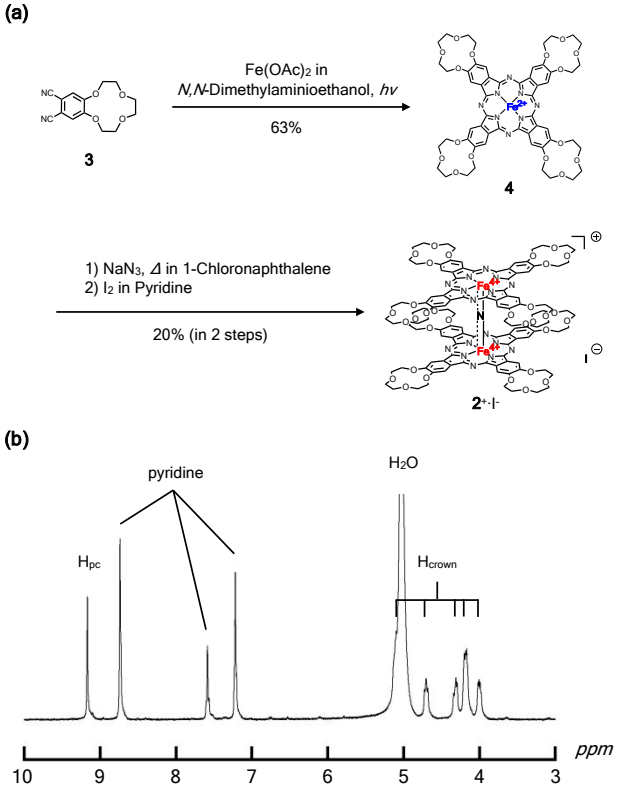


**Figure 2** (a) Synthesis of **2**$^+$·I$^-$. (b) $^1$H-NMR spectrum of **2**$^+$·I$^-$ in pyridine-$d_5$.

MALDI-TOF MS showed signals at around *m/z* = 2318.7, which correspond to those of the calculated isotope pattern for **2**$^+$ (Figure S3). In the $^1$H-NMR spectrum (Figure 2b), sharp signals were assigned as $C_4$-symmetrical species. A neutral species of a μ-nitrido-bridged iron phthalocyanine dimer containing Fe(III) and Fe(IV) centers exhibits a significant broadening of $^1$H-NMR signals with paramagnetic shifts due to the *S* = 1/2 spin in the iron center.[21] In contrast, a monocationic species with two Fe(IV) centers shows sharp $^1$H-NMR signals.[17,18,21,22] Therefore, we concluded that **2**$^+$·I$^-$ contains two Fe(IV) centers interacting with each other in an antiferromagnetic fashion. The other characteristic feature of the $^1$H-NMR spectrum of **2**$^+$·I$^-$ is that the two germinal protons of each $CH_2$ group of 12-crown-4 units were observed as two different signals. This is because the chemical environments of these two germinal protons became different in a cofacial assemblage of two iron phthalocyanines connected to each other through a nitrogen atom. As for the UV-Vis spectrum of **2**$^+$·I$^-$, peaks corresponding to Q-bands of the phthalocyanine rings were observed at 588, 645, and 683 nm (Figure S4).

(a)

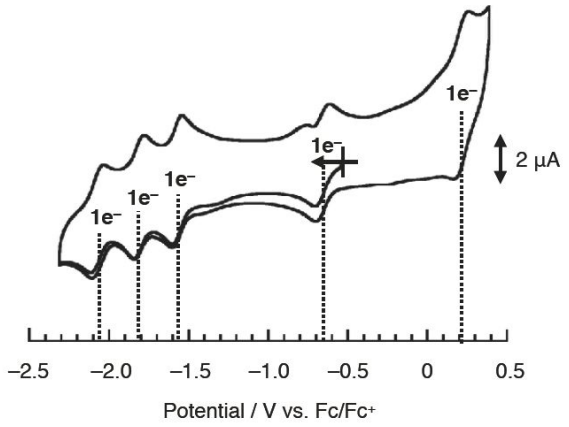


(b)

| Redox reaction | $1^{+\cdot}I^-$ | $2^{+\cdot}I^-$ |
|---|---|---|
| $M^{2+}$ / $M^+$ | 0.36 | 0.22 |
| $M^+$ / M | −0.58 | −0.66 |
| M / $M^-$ | −1.52 | −1.57 |
| $M^-$ / $M^{2-}$ | −1.74 | −1.81 |
| $M^{2-}$ / $M^{3-}$ | −2.00 | −2.07 |

M : neutral species (**1** or **2**)

**Figure 3** (a) Cyclic voltammogram of $\mathbf{2}^{+\cdot}I^-$ (200 μM) in a pyridine solution containing 100 mM of $^n Bu_4N^+ \cdot PF_6^-$ at room temperature. [scan rate] = 100 mV/s. (b) Comparison of the redox potentials (V vs. Fc/Fc$^+$) of $\mathbf{1}^{+\cdot}I^-$ (ref. 20) and $\mathbf{2}^{+\cdot}I^-$.

A cyclic voltammogram of $\mathbf{2}^{+\cdot}I^-$ was measured in a pyridine solution (200 μM) containing 100 mM of $^n Bu_4N^+ \cdot PF_6^-$ and compared with that of a monocationic μ-nitrido-bridged iron phthalocyanine dimer with no peripheral substituents ($\mathbf{1}^{+\cdot}I^-$), as shown in Figure 3a. Five quasi-reversible 1e$^-$ redox waves were observed at −2.07, −1.81, −1.57, −0.66, and 0.22 V *vs.* Fc/Fc$^+$ in the potential range from −2.5 to 0.5 V. Four reductions at −2.07, −1.81, −1.57, and −0.66 V can be assigned as those of the two iron centers based on a previous report by C. Ercolani *et al*. on the redox mechanism of $\mathbf{1}^+$.[24] One oxidation wave at 0.22 V should be the redox of the phthalocyanine ring. Importantly, a comparison of the voltammograms of $\mathbf{1}^{+\cdot}I^-$ and $\mathbf{2}^{+\cdot}I^-$ revealed that all five redox signals showed negative shifts, [21] as shown in Figure 3b, clearly indicating the electron-donating character of the peripheral 12-crown-4 units.

Heterogeneous methane oxidation reactions using silica-supported catalyst $\mathbf{2}^{+\cdot}I^-/SiO_2$ and $\mathbf{1}^{+\cdot}I^-/SiO_2$ were performed in an aqueous solution containing excess $H_2O_2$ (189 mM) and TFA (51 mM) at 60 °C. It is known that $\mathbf{1}^+$ affords high-valent oxo species ($\mathbf{1_{oxo}}$) in this reaction condition.[15-17] The amounts of the oxidized products (methanol, formaldehyde, and formic acid) were determined by GC-MS analyses. To evaluate the methane oxidation activity of the catalysts, the effective total turnover numbers ($TTN_{eff}$) defined by equations (i) and (ii) were calculated. $TTN_{eff}$ is based on the idea that methane is oxidized in a stepwise manner, as shown in Figure 1a.

$$TTN_{eff} = TTN(CH_4) - TTN(N_2), \quad \text{(i)}$$

$$TTN(CH_4) \text{ or } TTN(N_2) = (C_{Methanol} + 2 \times C_{Formaldehyde} + 3 \times C_{Formic\ acid}) / C_{Cat} \quad \text{(ii)}$$

Significant amounts of methanol, formaldehyde, and formic acid were detected during the course of the oxidation for both of $\mathbf{2}^{+\cdot}I^-/SiO_2$ and $\mathbf{1}^{+\cdot}I^-/SiO_2$ as shown in Table 1 and Figure S5. The fact that the $TTN_{eff}$ was increased suggests that methane was actually oxidized by these catalysts in this reaction condition. The $TTN_{eff}$ of $\mathbf{2}^{+\cdot}I^-/SiO_2$ after 4 h of oxidation was found to be larger than that of $\mathbf{1}^{+\cdot}I^-/SiO_2$ under the same reaction conditions (Table 1, entry 2 and entry 6).

However, apparent bleaching of the color of the phthalocyanine was observed especially after 6 h only in the case of $\mathbf{2}^{+\cdot}I^-/SiO_2$, indicating that catalyst $\mathbf{2}^+$ gradually decomposed during the reaction. Actually, the amount of the oxidized products by $\mathbf{2}^{+\cdot}I^-/SiO_2$ was also considerably larger than those for $\mathbf{1}^{+\cdot}I^-/SiO_2$ even in the absence of methane (under $N_2$) (Figures S5 and Table S1). This suggests that these oxidized products were also generated from the catalyst $\mathbf{2}^+$. We attribute that the oxidized products observed in the reaction by $\mathbf{1}^{+\cdot}I^-/SiO_2$ under $N_2$ condition were originated from the

**Table 1.** Oxidation of methane by μ-nitrido-bridged iron phthalocyanine dimer-based catalysts on silica supports.

| Entry | Catalyst | Reaction Time / h | Gas | Additive | $[CH_3OH]$ / mM | [HCHO] / mM | [HCOOH] / mM | $TTN_{eff}$ |
|---|---|---|---|---|---|---|---|---|
| 1 | $\mathbf{2}^{+\cdot}I^-/SiO_2$ | 2 | $CH_4$ (1.0 MPa) | ••• | 0.03 | 0 | 0 | 0 |
| 2 | $\mathbf{2}^{+\cdot}I^-/SiO_2$ | 4 | $CH_4$ (1.0 MPa) | ••• | 0.07 | 0.11 | 0.03 | 6 |
| 3 | $\mathbf{2}^{+\cdot}I^-/SiO_2$ | 6 | $CH_4$ (1.0 MPa) | ••• | 0.15 | 0.33 | 0.22 | 27 |
| 4 | $\mathbf{2}^{+\cdot}I^-/SiO_2$ | 8 | $CH_4$ (1.0 MPa) | ••• | 0.14 | 0.24 | 0.27 | 26 |
| 5 | $\mathbf{2}^{+\cdot}I^-/SiO_2$ | 6 | $CH_4$ (1.0 MPa) | 100 mM $Na_2SO_3$ | 0.11 | 0.05 | 0 | 4 |
| 6 | $\mathbf{1}^{+\cdot}I^-/SiO_2$ | 4 | $CH_4$ (1.0 MPa) | ••• | 0.04 | 0 | 0.07 | 5 |

All reactions were performed in the presence of methane (1.0 MPa), $H_2O_2$ (189 mM), and TFA (51 mM) in $H_2O$ (3.0 mL) containing a silica-supported catalyst (55 μM as $\mathbf{2}^+$ or $\mathbf{1}^+$). Concentrations of the oxidized products are the mean values of three different reactions. The $TTN_{eff}$ values were calculated using equations (i) and (ii).

adsorbed organic solvents on $SiO_2$ surface, since it is known that $\mathbf{1}^+$ core is enough stable even in this reaction condition.[15-17] We also performed the oxidation reaction of $^{13}$C-labeled methane by $\mathbf{2}^{+}\cdot I^-/SiO_2$ in order to confirm the origin of the oxidized products. As shown in Figure S6, isotopic patterns of the mass spectra of the oxidized products were clearly changed from those observed in the reactions using unlabeled methane, indicating that part of these products were actually originated from methane. Considering the fact that $TTN_{eff}$ for $\mathbf{2}^{+}\cdot I^-/SiO_2$ began to increase after 2 h and reached a maximum at approximately 6 h (Figure 4a), the transiently generated species should have shown methane oxidation activity.

To confirm the possibility of the Fenton-type reaction, in which the hydroxyl radical (•OH) acts as a reactive species instead of a high-valent iron-oxo species, we performed an oxidation reaction in the presence of excess $Na_2SO_3$, a radical scavenger (Table 1, entry 5 and Table S1, entry 5).[9] As shown in entry 5 of Table 1, the $TTN_{eff}$ was significantly lowered in the presence of $Na_2SO_3$, indicating that methane oxidation by the transiently generated species should have proceeded via a Fenton-type reaction mechanism. In addition, the bleaching of the color of the catalyst was observed even in this case, implying that the decomposition of the catalyst center was not suppressed. Therefore, it is considered that the initially generated iron-oxo species of $\mathbf{2}_{oxo}$ is unstable and prone to decomposition. Taking these facts into consideration, we suggest a reaction mechanism of methane oxidation by $\mathbf{2}^{+}\cdot I^-/SiO_2$ as summarized in Figure 4b. It is interesting that apparent bleaching was not observed in the catalytic methane oxidation reaction using a μ-nitrido-bridged dinuclear iron complex of a supramolecular cofacial assembly of a porphyrin and a phthalocyanine connected through four 24-crown-8–dialkylammonium rotaxanes ($\mathbf{S}^{5+}\cdot 5Cl^-$ in Figure 1d), suggesting a high-valent iron-oxo species acted stably as a reactive species for methane oxidation in this case. We suppose that this difference in the reaction mechanism might be originated from the difference in the structures of porphyrinoids contained in the catalysts.

## Conclusions

We synthesized a novel monocationic μ-nitrido-bridged iron phthalocyanine dimer with eight 12-crown-4 units ($\mathbf{2}^{+}\cdot I^-$). $^1$H-NMR studies indicated that $\mathbf{2}^{+}\cdot I^-$ contains two iron (IV) ions interacting with each other in an antiferromagnetic manner because $\mathbf{2}^{+}\cdot I^-$ was observed as a diamagnetic species. The strong electron-donating ability of the peripheral eight 12-crown-4 units of $\mathbf{2}^+$ was confirmed by the fact that five redox signals in the cyclic voltammogram of $\mathbf{2}^{+}\cdot I^-$ shifted significantly to lower potentials compared to those of $\mathbf{2}^{+}\cdot I^-$. Although we first expected that the high-valent iron-oxo species of $\mathbf{2}^+$ possesses strong methane oxidation activity, a series of our methane oxidation experiments suggested that $\mathbf{2}^+$ is prone to decomposition during the reaction to afford transient species possessing methane oxidation activity. The introduction of 12-crown-4 units might have destabilized the high-valent iron-oxo species generated *in situ* under these reaction conditions. This result provides valuable information for designing a potent methane oxidation catalyst based on μ-nitrido-bridged iron phthalocyanine dimers.

## Experimental

**General** All reagents and solvents were purchased at the highest commercial quality available and used without further purification, unless otherwise stated. 4,5-dicyano-benzo-12-crown-4 (**3**) was prepared by slight modification of the procedure reported by C. Ma et al as described in the Supporting Information.[25] Synthesis of an iron phthalocyanine bearing four 12-crown-4 units (**4**) is described in the Supporting Information. A monocationic μ-nitrido-bridged iron phthalocyanine dimer with no peripheral substituents ($\mathbf{1}^{+}\cdot I^-$) was prepared according to our previous report.[20] $^1$H NMR spectra were recorded on a JEOL JNM-ECS400-A (400 MHz for $^1$H) spectrometer at a constant temperature of 298 K. Elemental analysis was performed on a Yanaco MT-6 analyzer. The absorption spectrum was recorded with a Hitachi U-4100 spectrophotometer in pyridine solutions at 20 ± 0.1 °C in 1.0 cm quartz cells. MALDI-TOF MS was performed on Bruker Daltonics ultraXtreme using α-CHCA as a matrix.

**Synthesis of $\mathbf{2}^{+}\cdot I^-$.** **4** (156 mg, 135 μmol), $NaN_3$ (86.0 mg, 1.32 mmol), and 1-chloronaphthalene (5.2 mL) were placed in a 50 mL flask. The mixture was refluxed under air at the bath temperature of 280 °C for 30 minutes. The reaction mixture was diluted with hexane (50 mL) and filtered. The resulting blackish green solid was washed with hexane (50 mL) and $H_2O$ (100 mL). After dried under vacuum at 60 °C, the crude product was dissolved in pyridine (500 mL). Iodine (122 mg, 0.962 mmol) was added. The resulting solution was stirred for 14 hours at room temperature, followed by evaporation of the volatile compounds. The residue was washed with $Et_2O$ (1 L) to remove the remaining iodine, and then, dried under reduced pressure. The crude product was purified by silica gel column chromatography (4.0 cm$\phi$ × 10.5 cm, hexane : $CHCl_3$ :

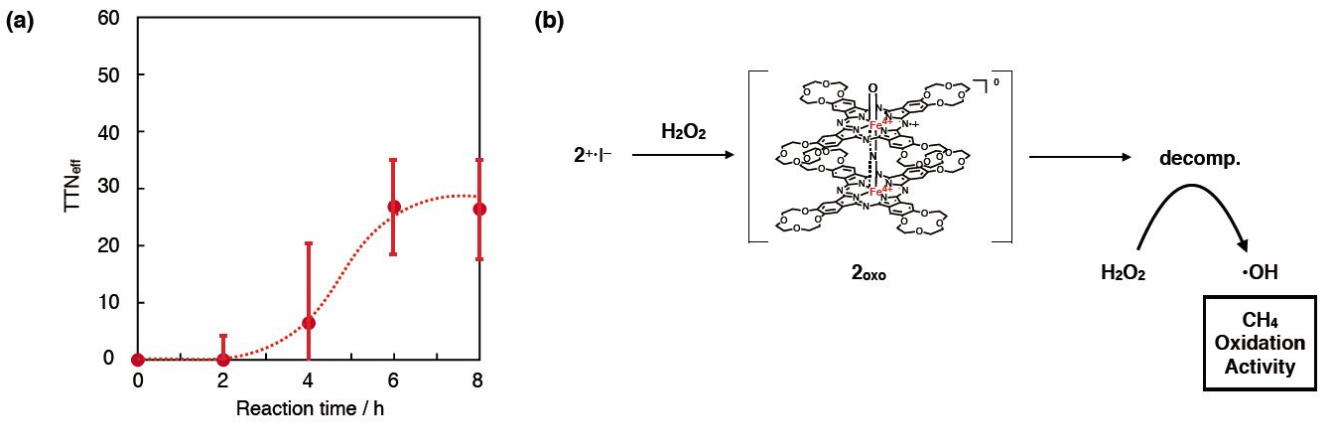


**Fig. 4** (a) Time dependence of $TTN_{eff}$ for methane oxidation by $\mathbf{2}^{+}\cdot I^-/SiO_2$. (b) Proposed mechanism of methane oxidation using $\mathbf{2}^{+}\cdot I^-/SiO_2$ in an acidic aqueous solution containing $H_2O_2$.

pyridine = 1 : 2 : 3) to give crude solid (88.7 mg), which was further purified by GPC (eluent : pyridine) to give the desired compound **6** as a dark green solid (35 mg, 15 μmol, 20%). $^1$H-NMR (400MHz, pyridine-$d_5$/TMS) : $\delta$ = 9.17 (*s*, 16H), 5.13-5.10 (*m*, 16H), 4.72-4.68 (*m*, 16H), 4.34-4.29 (*m*, 16H), 4.20-4.17 (*m*, 32H), 4.02-3.99 (*m*, 16H). MALDI-TOF MS : *m/z* = 2318.64: calcd for $C_{112}H_{112}Fe_2N_{17}O_{32}$ ([**2**]$^+$) found: 2318.69. Anal. Calcd. for $C_{112}H_{114}Fe_2IN_{17}O_{33}$ (**2**$^+$·I$^-$·$H_2O$): C; 54.58, H; 4.66, N; 9.66, Found: C; 54.45, H; 4.65, N; 9.74 (0.13% error).

**Preparation of silica-supported catalyst (2$^+$·I$^-$/$SiO_2$).** **2**$^+$·I$^-$ (41.6 mg, 16.9 μmol) was dissolved in 30 mL of pyridine. After the addition of silica gel (2.84 g) to the solution, the mixture was sonicated for 1 h. Pyridine was evaporated. $CH_2Cl_2$ (10 mL) was added to the residue, followed by sonication for 10 min. After $CH_2Cl_2$ was evaporated, the residue was dried under vacuum at 60 °C for 13 h. The catalyst was suspended in an aqueous TFA (TFA 6.0 mL + $H_2O$ 150 mL). The mixture was sonicated for 1 h and then the solid was filtered. This TFA wash procedure was repeated twice. Finally, the resulting solid was washed with $H_2O$ (100 mL × 3) and dried under vacuum at 60 °C for 19 h. The silica-supported catalyst was obtained quantitatively.

**Cyclic voltammogram of 2$^+$·I$^-$.** Cyclic voltammograms were measured with a BAS Electrochemical Analyzer Model 750Ds at room temperature in pyridine solutions containing 100 mM $TBAPF_6$ in a standard one-component cell under an $N_2$ atmosphere equipped with a 3 mm-O.D. glassy carbon disk working electrode, platinum wire counter electrode as Ag/AgCl reference electrode. All solutions were deoxygenated by $N_2$ bubbling for at least 20 min. Obtained $E^{\circ\prime}$ vs. Ag/AgCl were converted to those *vs.* $Fc/Fc^+$ based on measured redox potential of ferrocene. Tetrabutylammonium hexafluorophosphate ($TBAPF_6$) was recrystallized from 95% EtOH and dried under vacuum overnight at 100 °C.

**Methane oxidation reactions**. Oxidation of methane was performed in a stainless-steel autoclave with a glass tube. A mixture of the catalyst on $SiO_2$ (30 mg, 55 μM as **2**$^+$·**I**$^-$), TFA (12 μL, 51 mM), and 35% aqueous $H_2O_2$ (50 μL, 189 mM) in $H_2O$ (3.0 mL) was heated at 60 °C under 1.0 MPa of methane for 2–8 h. After the autoclave was opened, the reaction mixture was filtrated through a disposable membrane filter. The filtrate was analyzed by GC-MS (system: Agilent 7890A equipped with JEOL JMS-T100GCV, detection: EI, column: Agilent DB-WAX UI, external standard: isovaleric acid (5 mM), temperature conditions: initial: 70 °C to 220 °C (10 °C/min) – hold (5 min)). The yields of methanol and formic acid were determined based on the results of GC-MS. The yield of formaldehyde was examined using the method reported by Yu et al as reported in our previous paper.[17]

## Conflicts of interest

There are no conflicts to declare.

## Acknowledgements

This work was financially supported by a JSPS KAKENHI Grant-in-Aid for Scientific Research (A) (Number 19H00902) to KT, a JSPS KAKENHI Grant-in-Aid for Scientific Research (B) (Number 19H02787), JST PRESTO (Number JK114b) for YY.

## Notes and references

1 P. C. Bruijnincx and B. M. Weckhuysen, *Angew. Chem. Int. Ed.*, 2013, **52**, 11980-11987.

2 Z. Guo, B. Liu, Q. Zhang, W. Deng, Y. Wang, Y. Yang, *Chem. Soc. Rev.*, 2014, **43**, 3480–3524.

3 S. J. Blansby and G. B. Ellinton, *Acc. Chem. Res.*, 2003, **36**, 255.

4 M. Ravi, M. Ranocchiari, J. A. van Bokhoven, *Angew. Chem. Int. Ed.*, 2017, **56**, 16464–16483.

5 Z. Liang, T. Li, M. Kim, A. Asthagiri, J. F. Weaver, *Science*, 2017, **356**, 299–303.

6 B. E. R. Snyder, P. Vanelderen, M. L. Bols, S. D. Hallaert, L. H. Böttger, L. Ungur, K. Pierloot, R. A. Schoonheydt, B. F. Sels, E. I. Solomon, *Nature*, 2016, **536**, 317–321.

7 J. Shan, M. Li, L. F. Allard, S. Lee, M. Flytzani-Stephanopoulos, *Nature*, 2017, **551**, 605–608.

8 V. L. Sushkevich, D. Palagin, M. Ranocchiari, J. A. van Bokhoven, *Science,* 2017, **356**, 523–527.

9 C. Hammond, M. M. Forde, M. H. Ab Rahim, A. Thetford, Q. He, R. L. Jenkins, N. Dimitratos, J. A. Lopez-Sanchez, N. F. Dummer, D. M. Murphy, A. F. Carley, S. H. Taylor, D. J. Willock, E. E. Stangland, J. Kang, H. Hagen, C. J. Kiely, G. J. Hutchings, *Angew. Chem. Int. Ed.*, 2012, **51**, 5129–5133.

10 A. Hu, J.-J. Guo, H. Pan, Z. Zuo, *Science*, 2018, **361**, 668–672.

11 K. Ohkubo, K. Hirose, *Angew. Chem. Int. Ed.*, 2018, **57**, 2126–2129.

12 K. T. Smith, S. Berritt, M. González-Moreiras, S. Ahn, M. R. Smith III, M.-H. Baik, D. J. Mindiola, *Science*, 2016, **351**, 1424–1427.

13 P. Afanasiev, A. B. Sorokin, *Acc. Chem. Res.*, 2016, **49**, 583–593.

14 A. B. Sorokin, E. V. Kudrik, D. Bouchu, *Chem. Commun.*, 2008, 2562–2564.

15 E. V. Kudrik, P. Afanasiev, L. X. Alvarez, P. Dubourdeaux, M. Clémancey, J.-M. Latour, G. Blondin, D. Bouchu, F. Albrieux, S. E. Nefedov, A. B. Sorokin, *Nature Chem.*, 2012, **4**, 1024–1029.

16 Ü. ís¸ci, A. S. Faponle, P. Afanasiev, F. Albrieux, V. Briois, V. Ahsen, F. Dumoulin, A. B. Sorokin, S. P. de Visser, *Chem. Sci.*, 2015, **6**, 5063–5075.

17 Y. Yamada, K. Morita, N. Mihara, K. Igawa, K. Tomooka, K. Tanaka, *New J. Chem*., 2019, **43**, 11477–11482.

18 N. Mihara, Y. Yamada, H. Takaya, Y. Kitagawa, K. Igawa, K. Tomooka, H. Fujii, K. Tanaka, *Chem. Eur. J.*, 2019, **25**, 3369–3375.

19 Y. Gao, P. Ma, Y. Chen, Y. Zhang, Y. Bian, X. Li, J. Jiang, C. Ma, *Inorg. Chem.*, 2009, **48**, 45–54.

20 Y. Yamada, T. Sugiura, K. Morita, H. Ariga-Miwa, K. Tanaka, *Inorg. Chim. Acta*., 2019, **489**, 160-163.

21 L. A. Bottomley, B. B. Garrett, *Inorg. Chem.,* 1982, **21**, 1260-1263.
22 K. M. Kadish, R. K. Rhodes, L. A. Bottomley, H. M. Goff, *Inorg. Chem.,* 1981, **20**, 3195-3200
23 M. Li, M. Shang, N. Ehlinger, C. E. Schulz, R. W. Scheidt, *Inorg. Chem.,* 2000, **39**, 580-583.
24 L. A. Bottomley, J.-N. Gorce, V. L. Goedken, C. Ercolani, *Inorg. Chem.*, 1985, **24**, 3733–3737.
25 Y. Gao, P. Ma, Y. Chen, Y. Zhang, Y. Bian, X. Li, J. Jiang, C. Ma, *Inorg. Chem.*, 2009, **48**, 45–54.

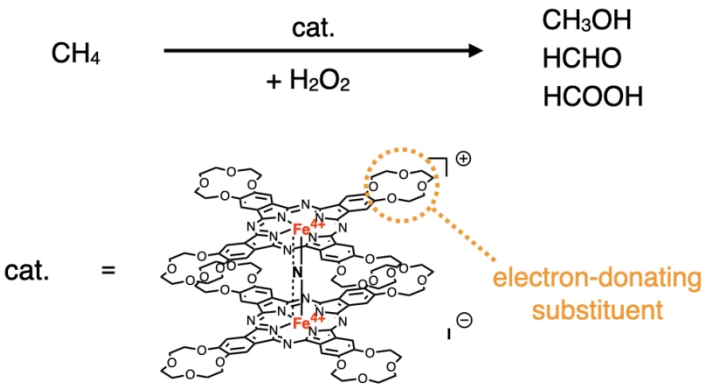


493x246mm (72 x 72 DPI)